



## Geophysical delineation of the geology and subsurface features of the Iramba area, central Tanzania, using aero-geophysical data with implications for mineral deposits

Peter Laizer<sup>1</sup> and Gabriel D Mulibo\*<sup>1</sup>

<sup>1</sup>Department of Geosciences, University of Dar es Salaam, P.O Box 35052, Dar es Salaam, Tanzania

Corresponding author: \*gabriel.mulibo@udsm.ac.tz

Received 20 Oct 2024, Revised 6 Feb 2025, Accepted 22 March 25, Published 14 April 2025

<https://dx.doi.org/10.4314/tjs.v51i1.8>

### Abstract

The Iramba area, known for its gold, base metal, and metallic mineral deposits, is not geophysically well exploited. The research presents an in-depth geophysical interpretation of the geology and the subsurface geological features and delineates hydrothermal alteration zones related to mineralisation in the area. The study involved detailed analysis and interpretations of high-resolution aero-geophysical data. Results from radiometric data have identified new granitic rocks and revealed a unique prominent feature in the region, which was previously not mapped. The identified new xenolith and foliated granites are characterised by high concentrations of all radiometric elements. The revealed prominent ring-like, NE trending feature is characterised by a high K concentration with moderate to high Th concentration. The feature shows significantly lower values of the Th/U ratios at the centre than the surrounding with intermediate magnetic signatures at the centre surrounded by high magnetic signatures. The study has also delineated zones of high K that coincide with low Th and Th/K ratio, indicating hydrothermally altered rocks and mineralisation in the area. The practical implications of this study are the future exploration and development of mineral resources for small-scale miners or larger-scale industrial mining in areas where mineralisations have been proposed.

**Keywords:** Iramba; Lithology; Alteration; Mineralisation; Aero-geophysical

### Introduction

The Iramba area lies within the Iramba–Sekenke greenstone belt (ISGB), which is one of the six Neoproterozoic greenstone belts located within the famous Lake Victoria Goldfields (LVGF) and is also known for its potential for gold and base metals deposits (Mkinga 1997; Kabete et al. 2012) (Figure 1). The ISGB lies in the most southeasterly of the Neoproterozoic greenstone belts within the Tanzania Craton. Over the past few decades, geological, geochronological, and geochemical data have contributed to the tectonic interpretation of the entire Iramba and the craton (Mkinga 1997; Kabete et al. 2012). However, most of the existing

interpretations in these studies are generally hampered by the lack of constraints on the surface and subsurface geometry of lithology and geological features due to the low resolution of the data. The available high-resolution aero-geophysical data in the area can provide accurate and helpful enhanced information on lithology and geological features.

Based on observations of the ground outcrops, it is sometimes difficult to accurately delineate lithological boundaries and reveal geological features because of the overburden or high inaccessibility of the area. Therefore, aero-geophysical approaches are the only methods that enhance the success of

conventional geological mapping (Boadi et al. 2013) and are needed to define and detect lithologies, geologic boundaries, hydrothermal activities, other subsurface geological features that are not identifiable by geological mapping (Hedenquist et al. 2000). The magnetic and radiometric surveys are capable, especially of locating and identifying the lithology and boundaries of the formations and the occurrence of metal ore deposits (Akinsunmade et al. 2020) and hydrothermal alteration zones (Airo 2002; Kumwenda and Lackie 2019).

Geophysical delineation of lithology offers insight into a better understanding of the surface and subsurface deep Earth related

to mineralisation (Airo 2002). The geophysical data are crucial in revealing contrasts in geophysical properties affected by lithological type, mineral types, alteration, crustal structure, subsurface geometry, and disposition (e.g., Airo 2002; Morgan 2012). These data can provide a link between outcropping rock, sediments, and the subsurface and map lithological boundaries and the unknown igneous bodies. Despite the availability of high-resolution geophysical data, the Iramba area has remained poorly investigated in term of geological features and lithological distributions associated with mineral deposits.

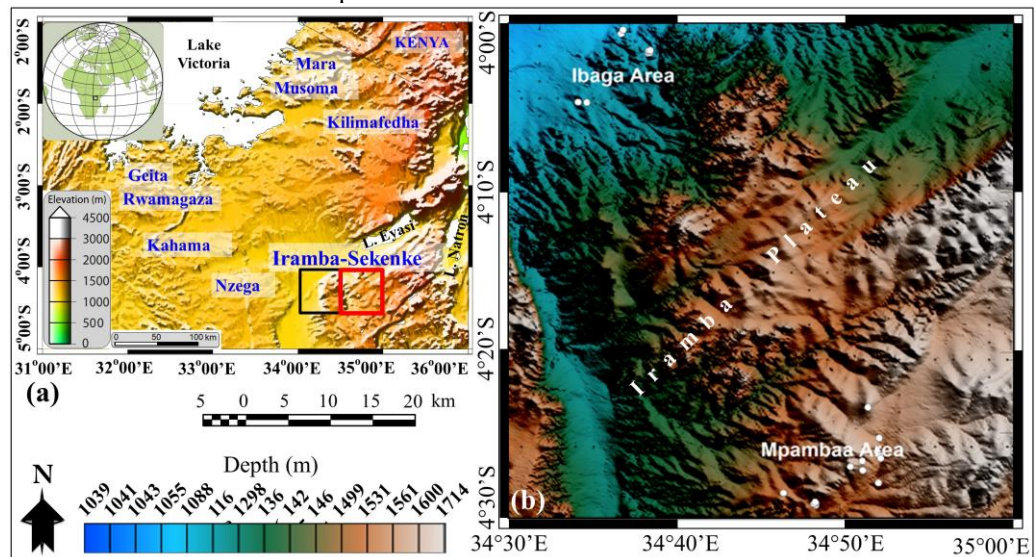


**Figure 1.** (a) A hill shaded map showing the Lake Nyanza Superterrane encompassing the Achaean greenstone belts within LVGF. The red rectangular insert is the study area enlarged as Figure 2. (b) Elevation map showing the study area. The white circles show the location of the artisanal mining areas.

Geophysical anomalies are usually related to the underlying basement rocks or igneous bodies within sedimentary layers (Gunn et al. 1997). These igneous rocks may serve as potential sources for a variety of minerals and heat, which may be utilised as guidance for the exploration of polymetallic deposits (e.g., Zighmi et al. 2023). The study area is well known to host gold and base metal mineralisation, which has been described to occur in quartz veins within the volcanic rocks at the contact between greenstone rocks

and diorite and the intersection between various linear structures, such as shear-fault, shear-dyke, fault-dyke, and dyke-dyke intersections (Laizer et al. 2024; Mkinga 1997; Ngole et al. 2016).

It is with this regard that this study uses high-resolution aero-geophysical data to remap the geology and delineate hydrothermal alteration zones and other geological features related to mineralisation in the Iramba area. The findings provide a new and significant insight into the

geological features, the distribution of hydrothermal alteration zones, and the improvement of the available and identification of new lithological boundaries in the Iramba area.

### The geology of the study area

The geology of the study area, located within the central Tanzania Craton, comprises mainly Neoarchaean granitoids, metasedimentary, and metavolcanic rocks (Moses et al. 2014) (Figure 2). The Neoarchaean magmatism started at about 2775 Ma and was not continuous due to interruption by crustal uplift and erosion of the older intrusives between 2712 and 2683 Ma, which resulted in the deposition of siliciclastic sediments with accompanying volcanism. The magmatic activity ended after approximately 160 years at about 2612 Ma (GST 2015), followed by the emplacement of smaller syenite plutons.

The volcano-sedimentary sequences were intruded by large granite plutons and

associated vein networks, which were later affected by deformation and accompanying low-grade metamorphism the effect, which is much revealed on folded granite veins. Though the tectono-metamorphic event is not known, it is assumed to take place before the emplacement of syenite plutons at about 2612 Ma (Ngole et al. 2016). The Iramba is also intruded by the regional NE-SW Palaeoproterozoic dolerite dykes swarm (Moses et al. 2014; Laizer et al. 2024). The dyke swarm has been preceded by the regional ductile shears, which in many cases are associated with gold mineralisation. The area also encompasses N-S basaltic dykes, which were emplaced during the Mesozoic time (Ngole et al. 2016). The Iramba area forms part of the elevated Iramba plateau and consists of the NNW–SSE Iramba faults (Figure 2). The Iramba plateau, to the northwest, consists of the NE-SW fault that borders the plateau from the Wembere depression.

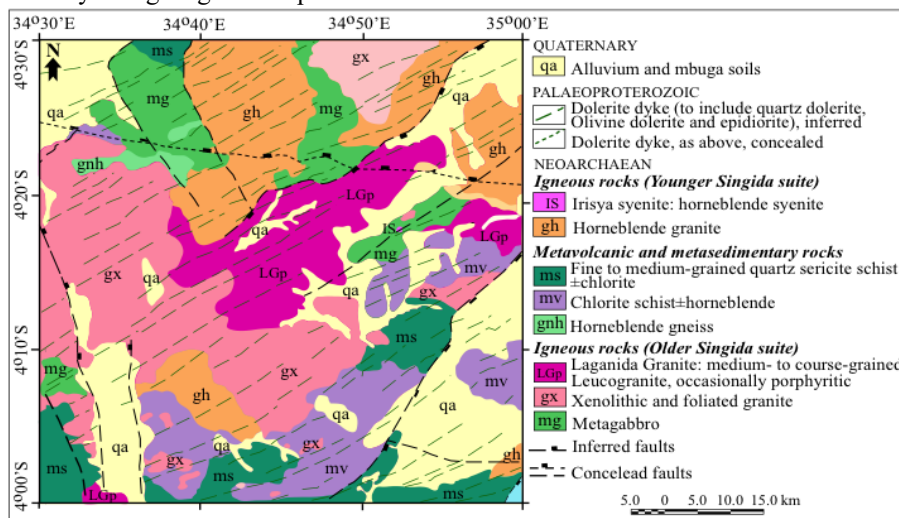


**Figure 2.** Geological map showing the chronological distribution of rocks in the study area (modified from Moses et al. 2014).

The lithostratigraphic sequence of the Iramba has been suggested to comprise granite-gneisses, the oldest rocks in the area, based on the higher degree of rock deformation, which is located in the north, west, central, and northeast of the study area (Mkinga 1997). The volcanic rocks and tuffs

and silvery schists that constitute the greenstone belt proper overlie the granite-gneisses. The lithostratigraphic relationship within the greenstone belt is further considered to consist of the volcanic rocks as the oldest rocks in the greenstone succession, which are carbonated and sheared, and the

less deformed show both vesicular and pillow structures (Mkinga 1997). The volcanic rocks are overlain by the banded iron formations (BIF), followed by the silvery schists of metasedimentary origin. The youngest lithological units in the area, lying in the northeastern, southwestern, and northeastern southwestern parts, consist of transported sediments of alluvium and mbuga soils deposited during the Quaternary (Moses et al. 2014).

## **Data and Methods**

### **Data acquisition**

The dataset used in this study is the high-resolution regional aero-geophysical (magnetic and radiometric) datasets acquired by Geotech Airborne Limited (VTEM) and Sander Geophysics Limited and provided by the Geological Survey of Tanzania. The aeromagnetic and radiometric data were acquired at a line spacing of 0.25 km and 2.5 km for the traverse line and tie line, respectively. The data were acquired using a flight altitude of ~60 m with traverse and tie line direction oriented N-S and E-W, respectively.

### **Data transformation and filtering**

To correct the temporal variation and regional effects and obtain the magnetic field of the crust, the diurnal corrections and the International Geomagnetic Reference Field (IGRF) were applied to the Total magnetic intensity (TMI) (Blakely 1996). The TMI data were gridded using the minimum curvature method (Briggs 1974; Lemna et al. 2018; Laizer and Mulibo 2024; Laizer et al. 2024) with a grid cell size of 65 x 65 m chosen based on the line spacing configuration, which is one-fourth of the survey line spacing to remove the artefacts perpendicular to the line direction (Dentith 2011). Reduced to the pole (RTP) transformation filter was used on the TMI to get the grid with symmetrical anomalies (Blakely 1996). The Automatic Gain Control (AGC) filter was applied to show the distribution of granitoid intrusion in the area (Rajagopalan and Milligan 1994). The filter was chosen to enhance the signal in areas of low field variability and reduce signal

amplitude in places of high variability by removing the background components and then equalising the signal across the survey area. The filter highlights continuity of structures across areas with different intensity. It converts waveforms of variable amplitude into waveforms of semi-constant amplitude and produces the data that give equal emphasis to signals with both low and high amplitudes used to enhance regional geological structures in the study area.

The radiometric data was processed using different filters and enhancement techniques to remove noises. The K, Th, and U concentration images were generated using minimum curvature with a grid cell size of 65 x 65 m, which is one-fourth of the survey line spacing. A composite image colour model, where red is assigned to potassium concentration, green to thorium, and blue to uranium (RGB), was created using the Oasis Montaj software package. The mobilisation of individual radioelements in response to specific geochemical conditions makes radioelement ratios sensitive in locating areas of mineralisation (Morgan 2012). The study of potassium enrichment can lead to the selection of mineral exploration targets related to hydrothermal alteration (e.g., Airo 2002; Kumwenda and Lackie 2019). The alteration processes affect the level of radiometric element concentration and mineralogical content (Airo 2002), and as such, they can be delineated using radiometric data as well as magnetic data (Elkhateeb and Abdellatif 2018; Kumwenda and Lackie 2019; this study).

The potential biases or limitations, which could affect radiometric signatures, include variability due to weathering or topographic effects. Where sediments are relatively thick, the radiometric signature of the underlying bedrock cannot be determined from the ternary image. In such areas, the variations in magnetic anomaly maps were used to infer the underlying bedrock lithology and structure. The location of areas in extensive but variable weathering results in large variations in colour tones within the same lithological boundaries, which could affect the interpretations; however, broadly

consistent areas can and have been defined.

## Results and discussion

### Lithological units from magnetic data

The lithological interpretation using magnetic data is based on RTP and AGC maps (Figure 3a and b). From RTP and AGC maps, three different magnetic zones have been interpreted. The first zone consists of LS1 and LS2 associated with alluvium and mbuga soils, metasediments, metavolcanic, and some granites as they contain more than 60% quartz. The second zone is characterised by IS associated with hornblende granite, hornblende gneiss, and metagabbro, which contain high ferromagnesian with low

amounts of felsic minerals. The third zone encompasses HS related to metagabbro, hornblende granite, xenolith and foliated granites and Laganida granite: medium- to coarse-grained leucogranite, occasionally porphyritic, which contains high ferromagnesian with a large amount of felsic minerals. The observed anomalies occur within the major NE-SW and minor N-S and NW-SE structural controlled trends. It is also important to note that a ring-like feature (RF) with an intermediate magnetic signature at the centre surrounded by high magnetic signatures occurs in the southern part (Figure 3).

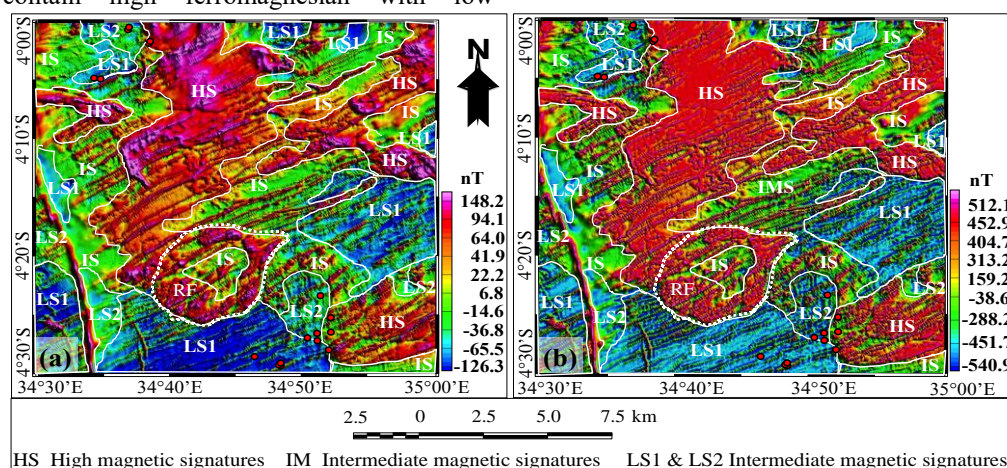


**Figure 3** Magnetic maps of (a) Reduced to the pole and (b) Automatic gain control showing the extension of granitoids and dyke swam. The red and blue colours indicate high and low magnetic intensities, respectively. The dashed polygon feature indicates the ring-like structure (RF).

### Lithological units from radiometric data

In this study, a ternary image of the radiometric data was interpreted (Figure 4), together with magnetic data (Figure 3) and information from field mapping, the existing geological map (Figure 2) to help identify and map continuous lithological units where possible across the study area. The image, to a large extent, correlates with the surface geology within the area, indicating a close spatial association with the rock units. The area contains various granitic rocks typically associated with pinkish and reddish tones, while greenish and bluish tones are associated with red sandy soil, mbuga.

The whitish colour on the ternary map of the study area covering the north, central and south, and some patches in the northeast, west and east, reflects rocks with high concentrations of K, Th and U radioelement such as gh, Lg and gx (Figure 4). These rocks are characterised by strong radiometric responses, which are differentiated from other rocks with low radioactive element concentrations. Some of the northwestern, eastern, and southwestern parts of the ternary map consist of dark colours, which are characteristic of rocks with low concentrations of K, Th, and U radioelements (Figure 4).

The reddish colour, covering most of the western part and parts of the northeast of the ternary map, represents high K content compared to Th and U. The reddish colour observed is due to the movement of radioactive elements concentration in the overburden caused by the high weathering process accentuated by topographic differences (Figure 1). These areas correlate with different types of granitoids, which include gh, Lg, and gx. In addition to the known granitic suites (gh, Lg, and gx), this study has identified two new xenolith and foliated granites (ga and g), which were previously not mapped. The greater part of

the southeastern section, minor parts of the southwestern, and some parts of the eastern section of the ternary map show bluish and greenish colours correlating with the regions of high Th and U with low K and are ascribed to qa and A1-A3. The intermediate green and blue colours coincide with the regions of intermediate Th and U with low K and correspond to ms and mv. Additionally, the dark colour, which occurs in patches in the northwestern, southwestern, and eastern parts of the study area, represents low Th, U, and K and correlates with mg and mv.

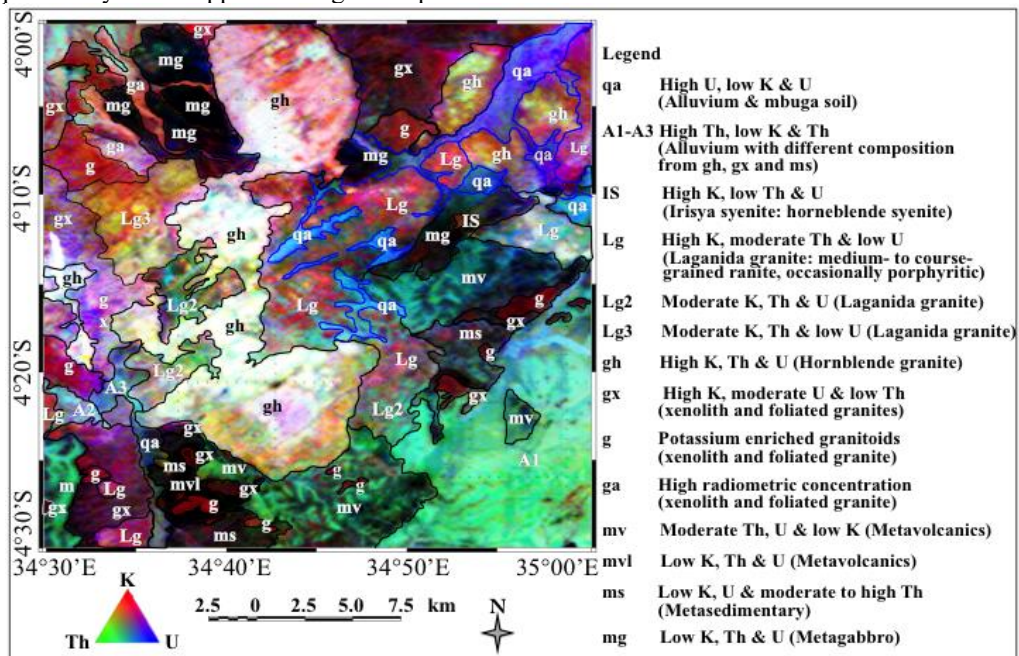


**Figure 4.** Ternary image with lithological units interpreted due to differences in concentration of radiometric elements.

The lowest concentration level in the total count contour map (Figure 5a) ranges from 25 to 900 counts/s and correlates with mg and mv. The moderate concentration level ranges from 1520 to 2545 counts/s, observed at the southern to southwestern, central to eastern, and northern parts of the study area, is related to mv, ms, and some of Lg, and gx. The high-level concentration in the range of 2545 to 3800 counts/s, observed at the central, west to northwest, part of the north, southeast, and northeast, is associated with gh, Lg, gx, and

qa. The lowest concentration level (0.3–0.9%) in the K contour map (Figure 5b) correlates with mg and some metavolcanics (mv). While the ms, qa, and some of mv and gx have moderate levels (1.0–2.4%), gh, Lg, and gx have the highest ones (2.5–4.2%). The Th contour map (Figure 5c) indicates that mg has the lowest concentration level. The highest level reaches 25 ppm and is associated with gh, Lg, gx, and qa, while mv and some of gh, gx, Lg, and ms have a



### **Magnetic and radiometric ratios associated with hydrothermal alteration zones and other geological features**

The known areas of gold mineralisation were overlain on the map with white circular shapes where most of these locations are controlled by NE-SW oriented structures, and some of the mineralisation occurs on the hydrothermally altered zone, a good indicative feature for gold occurrence (Figure 3). The interpreted zones of low magnetic signatures, characterised by the high density of faults and dykes, strongly indicate the presence of hydrothermally altered rocks within the study area. The low magnetic signature characterised by the highest concentration of geological structures (i.e., faults, fractures, and some dykes), as has been indicated in this study (Figure 3), represents, as compared with other regional geophysical studies, a typical characteristic feature in many regions affected by hydrothermal alterations (Kumwenda and Lackie 2019) and is thus clear evidence of alteration in the study area. It has been shown from other similar studies that hydrothermal processes affect the magnetic mineralogy and radiometric content of the deformed lithological units (Airo 2002), where their anomalies are depicted in magnetic and radiometric data (Kumwenda and Lackie 2019).

The radiometric elements U and Th are actinide elements with similar geochemical characteristics, and K is an alkaline element with different geochemical properties. Thus, during hydrothermal alteration, the addition of Th in the rock does not accompany K (e.g., Kumwenda and Lackie 2019), and the K concentration is much affected compared to other radioactive elements as it is added to the host rocks through mineralised hydrothermal fluids (Airo 2002). In areas where there is high K enrichment, low to moderate Th and very low Th/K ratios

indicate potassium alteration (Shives et al. 2000) and potentiality for gold deposits (e.g., Dickson and Scott 1997; Airo 2002; Kumwenda and Lackie 2019; Laizer and Mulibo 2024). The areas with low Th/K indicated by dashed white outlines (Figure 6a), coinciding with high K (Figure 5b) and low Th anomalies (Figure 5c), indicate possible hydrothermal alteration zones in the study area. From the map of the Th/K ratio (Figure 6a), the areas affected by the hydrothermal process correlate with gh, gx, ms, and mv in the northeastern, northwestern, and eastern parts of the study area (Figure 7).

In addition to alteration zones, a prominent feature has also been observed in the southern part (Figure 6b). The feature has a high concentration of K with moderate to high concentrations of Th and U (Figures 4b-d), but the ratio of Th/U (Figure 6a) at the centre of the feature is near 1.36 and significantly lower than its surroundings (Th/U: 6.61 to 15). The feature also clearly appears in the magnetic data, which shows a ring-like feature trending in NE with intermediate magnetic signatures at the centre surrounded by high magnetic signatures (Figure 3). The radiometric distribution of the feature could be attributed to the reduction in Th in the centre of the observed feature relative to its surroundings. This implies that the centre of the observed feature is more homogeneous, and the geological processes have not relatively affected it. Various geological processes may have affected the inhomogeneous surrounding areas, which could have resulted in the rocks being metamorphosed or fractured (Elkhateeb and Abdellatif 2018). The surrounding is associated with the process of settling sulfide minerals at the bottom of the magma-cooled bodies (intrusions), forming a thin, high-grade layer of igneous deposits (Zighmi et al. 2023).

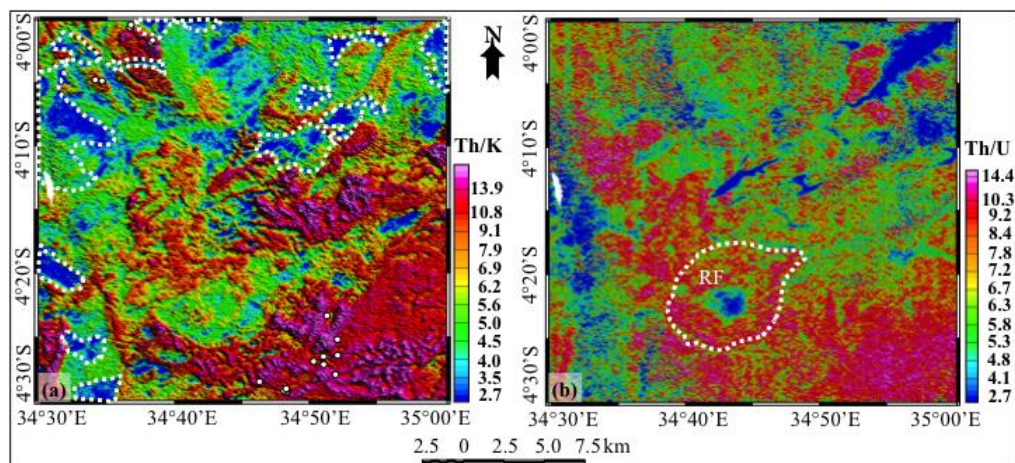


**Figure 6.** (a) Ratio images of Thorium and Potassium (Th/K) with the location of active and abandoned mines (white circles) within the study area showing hydrothermal alteration zones (dashed lines). (b) Thorium-Uranium (Th/U) ratio map showing the low to very low concentration of Th/U within the observed prominent feature surrounded by a high concentration of Th/U ratio.

### **Integration of the results and its economic and environmental impacts of mineralisation zones and implications for regional studies**

The produced lithological map (Figure 7), compared with the previous geological map presented by Moses et al (2014) (Figure 2), indicates that there is a close correlation between the indicated radioactive elements concentration and the corresponding rock units. The rock units gh, Lg, gx, mg, mv and ms, in the map, traced from the radiometric elements represent the basement complex, which correlates well with the rock units from the previous geological map. The differences observed, particularly in granitoids, between the two maps are due to the effect of extensive weathering and transportation of materials, resulting in large variations in colour tones within the same lithological boundaries. The results from both radiometric and aeromagnetic anomalies show elongation features trending NE-SW, NW-SE, and N-S, some of which are potential zones of mineralisation (Figures 6 and 7). Different from the previous map (Figure 2), the integrated lithological map (Figure 7) presents some lithological units, which were not previously geologically mapped, which include alluvium of A1-A3

type; metavolcanic rocks of mvl; granites presented as g and ga types (Figures 2 and 7). The proximity between the known mineralisation locations (mine areas) and the interpreted hydrothermal alteration zones in the northern part and other alteration zones not close to mine areas sheds light on mapped features that may be new promising sites (Figures 6 and 7).

From the composite map (Figure 7), the study area is characterised by metavolcanic and metasedimentary rocks, which are intruded by a porphyritic microcline of granite. The field observation shows that the majority of the gold deposits in the area lie in the volcanic series that are mainly composed of altered basalts and dolerites in the vicinity of the granitic contacts (Figure 7). The boundary between intrusive granitic rocks and the ductile greenstone sequences could depict areas of heterogeneous stress and unbalanced strain conditions (Robert et al. 2005). This implies that the competence contrast between the granitic rocks and the adjacent meta-sedimentary rocks provided favourable environment for gold and base metal deposition in the quartz veins within structures and shears as have also been shown in other regional studies (Duuring et al. 2007). The contacts between the intrusive

granites and the volcano-sedimentary rocks in the study area, alongside the presence of faults and shear zones (Figure 7), therefore, represent effective conduits of ore-fluid infiltration and gold depositional traps (Groves et al. 1998). This implies that intrusive granitic rocks in the study area have spatial and temporal associations with gold mineralisation. The intrusive rocks provided thermal energy that triggered the circulation of auriferous hydrothermal fluids resulting into gold mineralisation, and metallic minerals such as Cu, Zn, and Pb mineral deposits (e.g., quartz veins, diorite) (Zighmi et al. 2023). The Au-Cu-Pb-Zn anomalies have been shown to occur in the study area (Ngole et al. 2016), which appear to also have a deep-rooted source (Manya and Maboko 2008).

It has been suggested that several parallel sheared quartz veins in the Iramba-Sekenke greenstone belt (ISGB) contain gold values of interest close to the contact between greenstone and diorite (Mkinga 1997; Laizer et al. 2024). This phenomenon has been observed in several mines within the study area, that whenever there is a granite intrusion close to the ore zone, comparatively high grades at the contact between the intrusion and the meta-sediment occur, extending at a width in the range of 0.5-2.5 m. The extended width of economic mineralisation in other regional studies produced by intrusions through alteration or heating in the pre-existing rocks is within the revealed extension of up to 6 km from the margin (Duuring et al. 2007).

The potential proposed mineralisation zones could be further explored into discovery of mineral deposits suitable for mining activities for small-scale miners and large-scale mining. The discovery of the mineral deposits in the mineralised zones could benefit the country and the East Africa region through economic development by providing employment opportunities. The identified potential mineralised zones in the study area have a great economic impact of producing high yields of tones. The exploration of gold and other metallic minerals in the Iramba greenstone belt has the

potential of producing high-grade vein deposits that support small tonnage mining operations (Henckel et al. 2016) and is capable of producing greater than 0.5 M ounces of gold (Kabete et al. 2012). The gold, in one of the active mines, mined by small-scale miners has been shown to have a grade of ore in the range of 1.2 g/t to 2.58 g/t (e.g., Ngole et al. 2016).

The environmental impact from the mining activities on the mineralised zones results in the disturbance of the landscape, leading to loss of valuable land, natural trees and pasture for livestock. The mining activities can also result in decreased surface water storage due to mine tailings, which increase sediment load in the vicinity of rivers. A large amount of land is disturbed, and great quantities of waste are generated during the mining, resulting in erosion due to their instability, and the contaminated sediments are deposited in low land by rivers. The extraction of minerals, particularly heavy metals, results in the soil and water pollution in the area. These impacts have been observed in various mining activities around the country, such as the Kirondatal mine located in the Iramba-Sekenke greenstone belt (Mkinga 1997).

The findings in this study have vital implications for the regional geophysical studies in which the delineated granitic rocks and the potential sites for mineralisation due to K alteration provide a base for exploration in other areas. Similar regional studies that have been conducted in other areas around the globe using the same geophysical methods include the Tasiast mine located in the Reguibat Sield in Northern Mauritania within the Aouéouat Archean Greenstone Belt and the Um Salim gold mine in the Eastern Desert of Egypt (El-Sadek 2009; Heron et al. 2016). Results from their studies showed that the area is characterised by moderate to high magnetic anomalies and revealed areas of low- to moderate radiometric anomalies and enrichment of potassium interpreted as potassic alteration zones that could be associated with hydrothermal activity and mineral deposits.

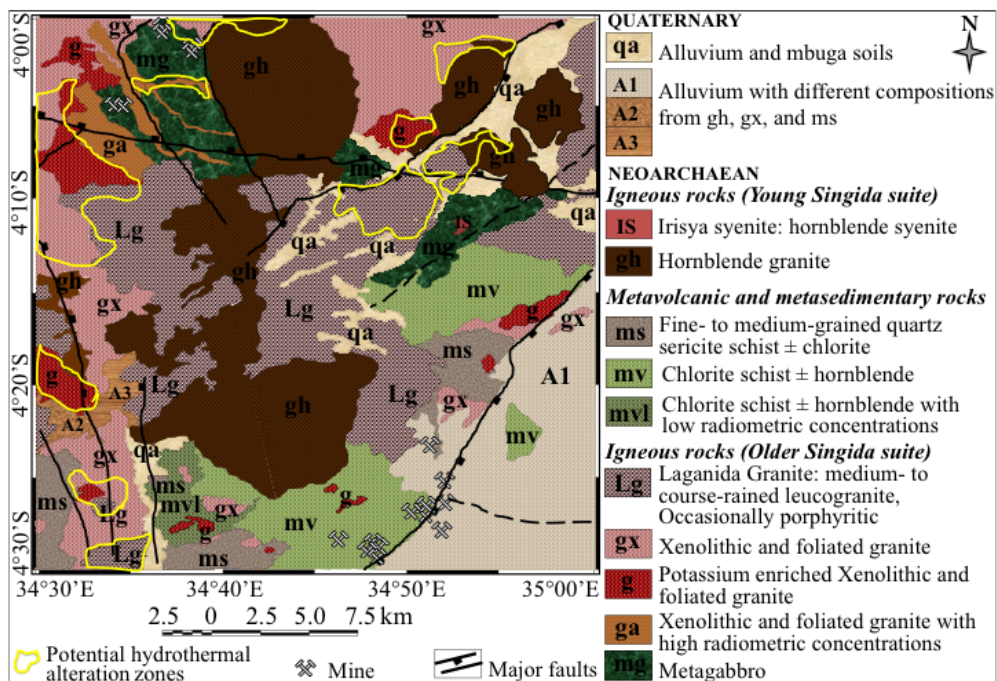


**Figure 7.** An interpreted composite map from aeromagnetic, aeroradiometric, and geological data, showing lithology and potential hydrothermal alteration zones.

## Conclusions

The interpretation of magnetic and radiometric data in this study provides insight into the geology and subsurface features of Iramba, particularly areas affected by hydrothermal activities, which provide vital information on the mineralisation of the area for future mineral exploration. The regions represented by the high magnetic anomaly and high K content compared to Th and U correlate with different types of granitoids that include gh, gx, and Lg. The interpreted magnetic and radiometric lithological map presents some lithological units, which were not previously geologically mapped. The observed zones of low magnetic signatures and high K that coincide with both low Th and Th/K are a strong indication of hydrothermally altered rocks and mineralisation in the area. Therefore, to understand the extent of the identified altered zones and the cause of alteration and ascertain the relationship between the granitoid and the alteration zones, further gold and Zn and Cu mineral exploration has

to be conducted in potential areas of hydrothermal alteration.

The prominent ring-like NE trending feature has, for the first time, been identified in the southern part of the study area, characterised by the high concentration of K with moderate to high concentrations of Th. The feature shows significantly lower values of the Th/U ratio at the centre, implying the centre forms a thin, high-grade layer of igneous deposits associated with the process of settling sulfide minerals at the bottom of the magma-cooled bodies. This feature does not appear on the geological map of Iramba and needs to be thoroughly investigated. This study, therefore, is of prime importance for small-scale miners and provides a way forward on opportunities for the discovery of deposits suitable for bulk mining. In the end, the impact of the explored subsurface mineralisation will contribute to the economic development of the country and the East Africa region, where employment will be generated and improve the lives of the local communities.

## Acknowledgements

The government of Tanzania, through the Geological Survey of Tanzania (GST) under the Ministry of Minerals, funded this study. Sincere appreciation is extended to GST for logistical support during the fieldwork and for providing the geophysical dataset used in this work. We also thank the two anonymous reviewers for the constructive comments that have improved the manuscript.

## Declaration of Interest

No potential conflict of interest was reported by the author(s).

## References

- Airo L 2002 Aeromagnetic and aeroradiometric response to hydrothermal alteration. *Surv. Geophys.* 23: 273–302.
- Akinsunmade A, Dinh CN, Wojas A and Tomecka-Suchoń S 2020 Characterization of lithological zones of the Isanlu sheet 225, North Central Nigeria, using aerogeophysical datasets. *Appl. Geophys.* 68: 651–665.  
<https://doi.org/10.1007/s11600-020-00411-6>.
- Blakely RJ 1996 Potential Theory in Gravity and Magnetic Applications. Port Chester, 1, Cambridge University Press. Cambridge, New York, Melbourne, Sydney, p. 464.
- Boadi B, Wemegah DD and Preko K 2013 Geological and structural interpretation of the Konongo area of the Ashanti gold belt of Ghana from aeromagnetic and radiometric data. *Int. Res. J. Geol. Min.* 3(3): 124–135.
- Briggs IC 1974 Machine Contouring Using Minimum Curvature. *Geophys.* 39(1): 39–48.
- Dentith MC 2011 Magnetic Methods, Airborne. In: Gupta HK (Ed) *Encyclopedia of Solid Earth Geophysics SE-119*. Ency. Earth Science Series. Springer Neth., pp. 761–766.
- Dickson BL and Scott KM 1997 Interpretation of aerial gamma-ray surveys—Adding the geochemical factors. *AGSO J. Aust. Geol. Geophys.* 17: 187–200.
- Duuring P, Cassidy KF and Hagemann SG 2007 Granitoid-associated orogenic, intrusion-related, and porphyry style metal deposits in the Archean Yilgarn Craton, Western Australia. *Ore. Geol. Rev.* 32(1–2): 157–186.  
<https://doi.org/10.1016/j.oregeorev.2006.11.001>.
- Elkhateeb SO, and Abdellatif MAG 2018 Delineation potential gold mineralization zones in a part of Central Eastern Desert, Egypt using Airborne Magnetic and Radiometric data. *NRIAG J. Aust. Geophys.* 7(2): 361–376.  
<https://doi.org/10.1016/j.nrjag.2018.05.010>.
- El-Sadek MA 2009 Radiospectrometric and magnetic signatures of a gold mine in Egypt. *J Appl Geophys.* 67: 34–43.  
<https://doi.org/10.1016/j.jappgeo.2008.08.012>.
- Geological Survey of Tanzania 2015 Explanatory Notes of the Geology of Singida QDS 82, 83,101 & 102. *Geological Survey of Tanzania, Dodoma*.
- Groves DI, Goldfarb RJ, Gebre-Mariam M, Hagemann SG and Robert F 1998 Orogenic gold deposits: a proposed classification in the context of their crustal distribution and relationship to other gold deposit types. *Ore Geol. Rev.* 13(1-5): 7–27.
- Gunn PJ, Maidment D and Milligan PR 1997 Interpreting aeromagnetic data in areas of limited outcrop. *J. Aust. Geol. Geophys.* 17(2): 175–185.
- Hedenquist JW, Arribas AR and Gonzalez-Urien E 2000 Exploration for epithermal gold deposits, Chapter 7, In: Hagemann SG, Brown PE (Eds), *Gold in 2000: Society of Economic Geologists. Rev. Econ. Geol.* 13: 245–277.
- Henckel J, Poulsen KH, Sharp TP and Spora P 2016 Lake Victoria Goldfields. *Epis.* 39(2):135–154.
- Heron K, Jessell K, Benn K, Harris E and Crowley QG 2016 The Tasiast deposit, Mauritania. *Ore Geol. Rev.* 78: 564–572.  
<https://doi.org/10.1016/j.oregeorev.2015.08.02>.
- Kabete JM, Groves DI, McNaughton NJ and Mruma AH 2012 A new tectonic and temporal framework for the Tanzanian Shield: Implications for gold metallogeny and undiscovered endowment. *Ore Geol. Rev.* 48: 88–124.  
<https://doi.org/10.1016/j.oregeorev.2012.02.0.09>.
- Kumwenda J and Lackie M 2019 Geophysical interpretation of the geology

- of the Stanthorpe region using aeromagnetic, gravity and radiometric data. *Expl. Geophys.* 50(6): 1–14.
- Laizer P and Mulibo G 2024 Geophysical characterisation of subsurface structures in relation to gold mineralization in the Mpambaa area, SE of Iramba-Sekenke Greenstone Belt, Tanzania. *Med. Geosc. Rev.* 7: 69-88  
<https://doi.org/10.1007/s42990-024-00142-6>.
- Laizer P, Mulibo G and Marobhe I 2024 Subsurface linear structures and potential zones of mineralisation of the Iramba-Sekenke greenstone belt, central Tanzania with implications for the structural-controlled mineralisation. *J. Afr. Earth Sci.* 215: 105261.
- Lemna OS, Stephenson R and Cornwell DG 2018 The role of pre-existing Precambrian structures in the development of Rukwa Rift Basin, southwest Tanzania. *J. Afr. Earth Sci.* 150, 607–625.
- Manya S and Maboko MAH 2008 Geochemistry and geochronology of Neoproterozoic volcanic rocks of the Iramba-Sekenke greenstone belt, central Tanzania. *Prec. Res.* 163:265–278.
- Mkinga BAM 1997 *Geological and environmental study of Kirondatal gold mine on the Iramba Plateau*. MSc Thesis, University of Dar es Salaam, Tanzania.
- Morgan LA 2012 Geophysical Characteristics of Volcanogenic Massive Sulfide Deposits. Volcanogenic Massive Sulfide Occurrence Model. *Scientific Investigations Report 2010-5070, US Geological Survey, Reston, VA*, pp. 115–131.
- Moses F, Momburi P and Kidsheni D 2014 Geological Maps QDS 82 and QDS 83 (1:100,000). *Geological Survey of Tanzania, Dodoma*.
- Ngole TT, Kalimenze JD, Malya GJ et al 2016 Preliminary Background Geological Report of Demarcated areas for Artisanal and Small Scale Miners (ASSM) in Singida Region. *Geological Survey of Tanzania report, Dodoma*.
- Rajagopalan S and Milligan P 1994 Image enhancement of aeromagnetic data using automatic gain control. *Expl. Geophys.* 25(4): 173–178.
- Robert F, Poulsen KH, Cassidy KF and Hodson CJ 2005 Gold metallogeny of the Superior and Yilgarn Cratons. *Econ. Geol.* 100: 1001–1033.  
<https://doi.org/10.5382/AV100.30>.
- Shives RB, Charbonneau BW and Ford KL 2000 The detection of potassic alteration by gamma-ray spectrometry—Recognition of alteration related to mineralization Detecting Ore Using GRS and K Alteration *Geophys.* 65(6): 2001–2011.  
<https://doi.org/10.1190/1.1444884>.
- Zighmi K, Zahri F, Hadji R et al 2023 Polymetallic mineralisation hosted in the Neogene sedimentary strata of the Algerian Tellian Range: A comprehensive overview. *Min. Miner. Depos.* 17(2): 20–27.  
<https://doi.org/10.33271/mining17.02.020>.